Incorporating the source wavelet and radiation pattern into the internal multiple attenuation algorithm

Jinlong Yang and Arthur B. Weglein, M-OSRP, University of Houston*

SUMMARY

The inverse scattering series internal multiple attenuation (ISS IMA) algorithm (Araújo et al., 1994; Weglein et al., 1997) is modified and extended by incorporating the source wavelet and radiation pattern in order to enhance the fidelity of the amplitude and phase predictions of the internal multiple. The modified ISS IMA algorithm is fully data-driven to predict all first-order internal multiples for all horizons at once, without requiring any subsurface information. In synthetic data tests, for data produced by a point source with a wavelet, the amplitude and shape of the predicted internal multiples are significantly improved by incorporating the source wavelet deconvolution. For data generated by a general source with a radiation pattern, the prediction is further improved by incorporating the source wavelet and radiation pattern into the algorithm. Therefore, the modified ISS IMA algorithm produces more accurate results when the data are generated by a frequency and angle dependent source.

INTRODUCTION

In seismic exploration, seismic reflection events are classified as primary or multiple, depending on whether the energy arriving at the receiver has experienced one or more upward reflections, respectively. Methods for seismic imaging and parameter estimation (inversion) assume that the data contain only primaries. Multiples are considered to be noise because they can interfere with primaries and/or be misinterpreted as primaries. Hence, multiple removal is a prerequisite to seismic imaging and inversion.

This abstract will focus on internal multiple attenuation and will analyze and test the impact of incorporating the source wavelet and radiation pattern on internal multiple prediction. The ISS IMA algorithm was first proposed by Araújo et al. (1994) and Weglein et al. (1997). It is a fully data-driven and model-type independent algorithm (Weglein et al., 2003), and it predicts the correct traveltimes and approximate amplitudes of all internal multiples at all depths at once. Matson et al. (1999) extended the theory for land and OBC applications. Ramírez and Weglein (2005) discussed how to extend the ISS IMA algorithm from attenuation toward elimination of multiples. Herrera and Weglein (2013) developed the 1-D ISS internal multiple elimination algorithm for internal multiple generated by a single shallowest reflector and Zou and Weglein (2013) further derived a general form of the ISS internal multiple elimination algorithm.

The ISS IMA algorithm has certain data requirements: (1) removal of the reference wavefield, (2) an estimation of the source wavelet and radiation pattern, (3) source and receiver deghosting, and (4) removal of the free-surface multiples. The first three requirements can be obtained by Green's theorem methods (Zhang and Weglein, 2005; Mayhan et al., 2012; Tang et al., 2013) and the free-surface multiples can be removed by the ISS free-surface multiple elimination algorithm (Carvalho, 1992; Weglein et al., 2003; Yang et al., 2013). Green's theorem methods and the ISS free-surface multiple elimination algorithm are consistent with the ISS IMA algorithm, since all are multidimensional wave-theoretic preprocessing methods and do not require subsurface information.

The ISS IMA algorithm assumes that the input data are spike wave. In other words, the input data have been deconvolved. If the input data are generated by a source wavelet instead of by a spike wave, the predicted internal multiple has convolved at least three source wavelets. Hence, the source wavelet has a significant effect on the amplitude and shape of the predicted internal multiple. In this paper, to improve the amplitude and the shape of a predicted internal multiple, the ISS IMA algorithm is extended to accommodate a source wavelet.

In addition, the ISS IMA algorithm assumes an isotropic point source, i.e., it assumes that the source has no variation of amplitude or phase with take-off angle. A large marine air-gun array will exhibit directivity and produce variations of the source signature (Loveridge et al., 1984). In on-shore exploration, even if there is no source array, the source can have radiation pattern or directivity. That directivity has significant effects on multiple removal or attenuation and AVO analysis. In seismic data processing, it is important that we characterize the source array's effect on any seismic processing methods. Therefore, to further improve the effectiveness of the ISS IMA algorithm, it is extended to accommodate a source wavelet and radiation pattern. The synthetic data tests show that accommodating the source wavelet and radiation pattern can enhance the fidelity of the amplitude and phase predictions of internal multiples.

THEORY

The ISS IMA algorithm (Araújo, 1994; Weglein et al., 1997, 2003) for first-order internal multiple prediction in a $2D$ earth is given by

$$\begin{aligned} b_3(k_g,k_s,\omega) &= \frac{1}{(2\pi)^2}\int_{-\infty}^{\infty}\int_{-\infty}^{\infty} dk_1 e^{-iq_1(z_g-z_s)} dk_2 e^{iq_2(z_g-z_s)} \\ &\times \int_{-\infty}^{\infty} dz_1 b_1(k_g,k_1,z_1) e^{i(q_g+q_1)z_1} \\ &\times \int_{-\infty}^{z_1-\varepsilon} dz_2 b_1(k_1,k_2,z_2) e^{-i(q_1+q_2)z_2} \\ &\times \int_{z_2+\varepsilon}^{\infty} dz_3 b_1(k_2,k_s,z_3) e^{i(q_2+q_s)z_3}, \end{aligned} \tag{1}$$

where ω, k_s and k_g are temporal frequency and the horizontal wavenumbers for source and receiver coordinates, respectively. q_s and q_g are the corresponding vertical source and re-

ceiver wavenumbers, respectively. $q_i = sgn(\omega)\sqrt{\omega^2/c_0^2 - k_i^2}$ for $i = (g,s)$; c_0 is the reference velocity. z_s and z_g are the source and receiver depths; and z_i ($i = 1,2,3$) represents pseudodepth (vertical depth of the water speed migration). The parameter ε is introduced to insure that the relations $z_1 > z_2$ and $z_3 > z_2$ are satisfied.

From the first-order equation of the inverse scattering series $D = G_0^d V_1 P_0^d$ (Weglein et al., 2003), which can be represented explicitly in 2-D case as

$$D(x_g,\varepsilon_g,x_s,\varepsilon_s,\omega) = \int dx_1 \int dz_1 \int dx_2 \int dz_2 \; G_0^d(x_g,\varepsilon_g,x_1,z_1,\omega) V_1(x_1,z_1,x_2,z_2,\omega) P_0^d(x_2,z_2,x_s,\varepsilon_s,\omega), \quad (2)$$

where the data D have been deghosted and the reference wavefield and free-surface multiples have been removed. G_0^d and P_0^d are the direct reference Green's function and the direct reference wavefield, respectively.

For a unit source, $P_0^d = G_0^d$. We take a Fourier transform over x_s and x_g on both sides of equation 2 and define b_1 as

$$b_1(k_g,k_s,q_g+q_s) \equiv \frac{V_1(k_g,q_g,k_s,q_s,\omega)}{-2iq_g} = -2iq_s D(k_g,k_s,\omega), \quad (3)$$

where b_1 represents effective plane-wave incident data and $D(k_g,k_s,\omega)$ is the Fourier-transformed prestack data. The input b_1 are introduced into equation 1 after an uncollapsed Stolt migration (Weglein et al., 1997) that takes $b_1(k_g,k_s,q_g+q_s)$ into the pseudodepth domain, $b_1(k_g,k_s,z_i)$, by using the reference velocity, c_0. Then, the first-order internal multiples $D_3(k_g,k_s,\omega)$, which are predicted by the ISS IMA algorithm (equation 1), are obtained by

$$D_3(k_g,k_s,\omega) = (-2iq_s)^{-1} b_3(k_g,k_s,q_g+q_s). \quad (4)$$

For an isotropic point source, $P_0^d = A(\omega)G_0^d$. Fourier transforming over x_s and x_g on both sides of equation 2 gives

$$b_1(k_g,k_s,q_g+q_s) = -2iq_s D(k_g,k_s,\omega)/A(\omega), \quad (5)$$

where $A(\omega)$ is the source signature. After b_3 has been predicted by equation 1, the first-order internal multiple is achieved by convolving the source wavelet $A(\omega)$ back

$$D_3(k_g,k_s,\omega) = (-2iq_s)^{-1} A(\omega) b_3(k_g,k_s,q_g+q_s). \quad (6)$$

For a general source with a radiation pattern (e.g., a source array), the direct reference wavefield P_0^d for a 2D case can be expressed as an integral of the direct reference Green's function G_0^d over all air-guns in an array,

$$P_0^d(x,z,x_s,z_s,\omega) = \int dx' dz' \rho(x',z',\omega) G_0^d(x,z,x'+x_s,z'+z_s,\omega), \quad (7)$$

where (x,z) and (x_s,z_s) are the prediction point and source point, respectively. (x',z') is the distribution of the source with respect to the source locator (x_s,z_s). Using the bilinear form of Green's function and Fourier transforming over x, we obtain the relationship between ρ and P_0^d as

$$P_0^d(k,z,x_s,z_s,\omega) = \rho(k,q,\omega)\frac{e^{iq|z-z_s|}}{2iq} e^{ikx}. \quad (8)$$

On the other hand, the reference wavefield P_0^d can be solved from the measured data by using Green's theorem method (Weglein and Secrest, 1990).

Since $k^2 + q^2 = \omega^2/c_0^2$, q is not a free variable, hence, we can not obtain $\rho(x,z,\omega)$ in space-frequency domain by taking an inverse Fourier transform on $\rho(k,q,\omega)$. However, the projection of the source signature $\rho(k,q,\omega)$ can be achieved directly from the direct reference wavefield P_0^d in the f-k domain, where the variable k or q represent the amplitude variations of the source signature with angles.

Substituting the projection of the source signature ρ into equation 2 and Fourier transforming over x_s and x_g gives

$$b_1(k_g,k_s,q_g+q_s) = -2iq_s D(k_g,k_s,\omega)/\rho(k_g,q_g,\omega). \quad (9)$$

Further details of obtaining ρ can be found in Yang et al. (2013) and Yang and Weglein (2013). The first-order internal multiple is calculated from b_3,

$$D_3(k_g,k_s,\omega) = (-2iq_s)^{-1}\rho(k_g,q_g,\omega) b_3(k_g,k_s,q_g+q_s). \quad (10)$$

All above derivations are 2D cases, and they can be directly extended to 3D. From the derivations, we can see that the kernel of the ISS IMA algorithm (equation 1) is not change and the source wavelet and radiation pattern are imported by equations 5 and 9. The predicted internal multiples D_3 are also affected by the source wavelet and radiation pattern in equations 6 and 10. If the source wavelet is not incorporated into the ISS IMA algorithm, the amplitudes and shapes of the predicted internal multiples are not comparable with those of the internal multiples in the input data. To improve the effectiveness of the internal multiple prediction, the ISS IMA algorithm should be modified for its input and output by accommodating the source wavelet and radiation pattern. This accommodation can enhance the fidelity of the amplitude and shape of the predictions of internal multiples.

NUMERICAL TESTS

In this section, we will present the numerical tests of the internal multiple prediction for the data generated by a point source and a general source with a radiation pattern. The numerical tests are based on a $1D$ acoustic model with varying velocity and constant density, as shown in Figure 1. The synthetic data that are generated by the finite-difference method. The data have one shot gather with 2001 traces, and each trace has 301 time samples, with $dt = 5ms$. The trace interval is $5m$.

The source wavelet effect on internal multiple prediction

For the data generated by a point source, the internal multiple will be predicted by using the ISS IMA algorithm with and without source wavelet deconvolution. Figure 2 shows the input data and their corresponding predicted internal multiples. They are plotted using the same scale. In the input data, the first two strongest events are the primaries, and the other events are internal multiples. Figures 2(b) and 2(c) show the predicted internal multiples using the ISS IMA algorithm with and without source wavelet deconvolution. From Figures 2(b) and 2(c),

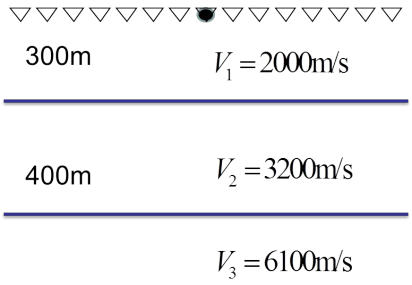

Figure 1: One-dimensional acoustic constant-density medium.

we can see that both algorithms predict the correct traveltimes, but they predict different amplitudes and shapes for the internal multiples. In Figure 2(b), the amplitude of the predicted internal multiple is comparable with the internal multiple in the input data, while the amplitude is totally different from that of the internal multiple in the input data in Figure 2(c).

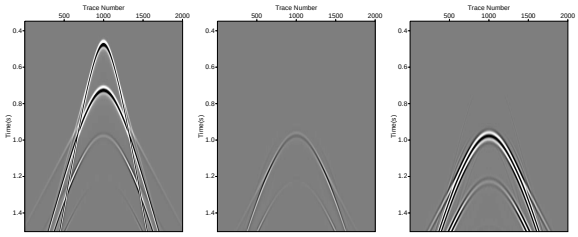

Figure 2: (a) The input data; (b) and (c) The internal multiples predicted by the ISS IMA algorithm with and without source wavelet deconvolution, respectively.

To see the details, we pick the middle trace (offset $= 0$) and the far trace (offset $= 1700m$) from each image in Figure 2. The time windows are chosen at $0.85s \sim 1.10s$ for the middle trace and at $1.05s \sim 1.25s$ for the far trace, as shown in Figure 3. For the middle trace, it can be seen that the shape of the internal multiple predicted by the ISS IMA algorithm without source wavelet deconvolution (Figure 3(c)) is totally different from that of the true internal multiple (Figure 3(a)). The predicted and true amplitudes are not comparable, either. This is because the predicted internal multiples convolve three wavelets. However, comparing Figure 3(b) with Figure 3(a), we can see that the amplitude and shape of the internal multiple predicted by the ISS IMA algorithm with source wavelet deconvolution are similar to those of the true internal multiple, as shown in Figure 4(a). It demonstrates that by accommodating the source wavelet deconvolution, the amplitude and shape of the predicted internal multiple are significantly improved for the internal multiple prediction. For the far-offset traces, we obtain the similar results, as shown in Figures 3(e) and 4(b).

From the numerical test, we conclude that by incorporating the source wavelet deconvolution, the ISS IMA algorithm produces more accurate and encouraging results for both zero offset and far offset. The predicted internal multiple has the correct traveltime, and the amplitude and shape are significantly improved. In addition, Liang et al. (2013) also discussed the source wavelet effect on the internal multiple prediction for the 1D normal incident model.

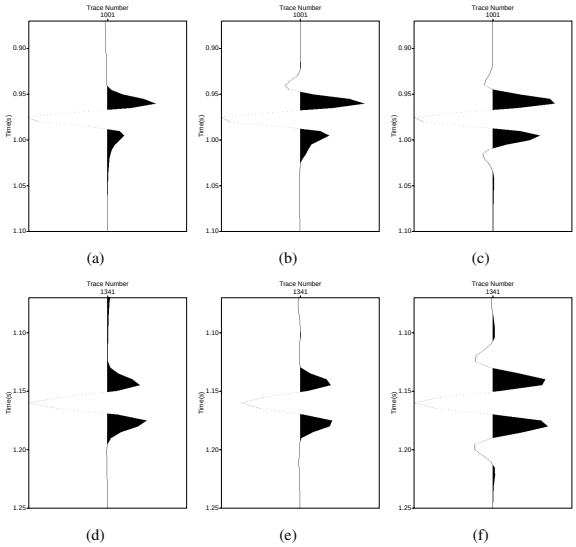

Figure 3: (a), (b), (c) The middle traces, and (d), (e), (f) the far traces, picked from the input data and the internal multiples predicted by the ISS IMA algorithm with and without source wavelet deconvolution.

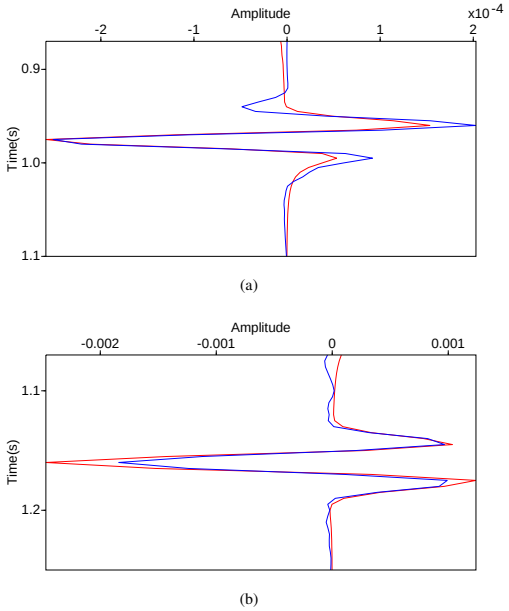

Figure 4: The comparison between the internal multiple (red) in the input data and the internal multiple (blue) predicted by the ISS IMA algorithm with source wavelet deconvolution at (a) zero offset and at (b) far offset ($1700m$).

The radiation pattern effect on internal multiple prediction

For the data generated by a general source with a radiation pattern (e.g., source array), we will predict the internal multiple using the ISS IMA algorithm with and without incorporating the source wavelet and radiation pattern. Here, the synthetic data are generated by a source array using the same model as Figure 1. The source array contains five point sources in one line with $20m$ range. Here, we assume that the source array only varies laterally with identical source signatures, but the assumption is not necessary in the ISS IMA algorithm.

Figure 5(a) shows the input data generated by the source array. Similar with the data generated by the point source, the first two strongest events are the primaries, and the other events are internal multiples. Figures 5(b) and 5(c) present the internal multiples predicted by using the ISS IMA algorithm with and without incorporating the source wavelet and radiation pattern. From Figures 5(b) and 5(c), we can see that both algorithms can predict the correct traveltime and an acceptable amplitude of the internal multiple.

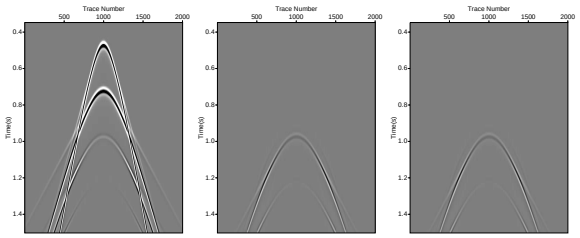

(a) (b) (c)

Figure 5: (a) The input data; (b) and (c) the internal multiples predicted by the ISS IMA algorithm with and without incorporating the source wavelet and radiation pattern.

To compare the internal multiple predictions in detail, the middle trace (offset $= 0$) and the far trace (offset $= 1700m$) are picked from each image in Figure 5. We choose the time windows at $0.85s \sim 1.10s$ for the middle trace and at $1.05s \sim 1.25s$ for the far trace, as shown in Figure 6. Comparing the middle and far traces, we can see that the amplitude and shape of the internal multiple predicted by the ISS IMA algorithm with and without incorporating the radiation pattern are very similar to those for the true internal multiple in the input data. Their comparisons are plotted in Figure 7. At zero offset, there are no visible differences, as shown in Figure 7(a), while at far offset, Figure 7(b) demonstrates that the amplitude of the internal multiple prediction is further improved by accommodating the radiation pattern. Therefore, for the general source data, the modified ISS IMA algorithm that incorporates the source wavelet and radiation pattern can enhance the accuracy and effectiveness of the amplitude prediction of the internal multiple.

CONCLUSIONS

The ISS IMA algorithm is modified and extended by accommodating the source wavelet and radiation pattern, which can be provided by the prerequisite. The ISS IMA modified algorithm enhances the fidelity of amplitude and phase predictions of the internal multiple. It retains all the merits of the original algorithm that is fully data-driven and does not require any subsurface information. In synthetic data tests, for data generated by a point source with a wavelet, the predictions of the amplitudes and shapes of internal multiples are significantly improved by incorporating the source wavelet deconvolution. For data generated by a general source with a radiation pattern, the prediction is further improved by incorporating the source wavelet and radiation pattern into the ISS IMA algorithm. We expect this extended ISS IMA algorithm to be relevant and useful for on-shore application, as well.

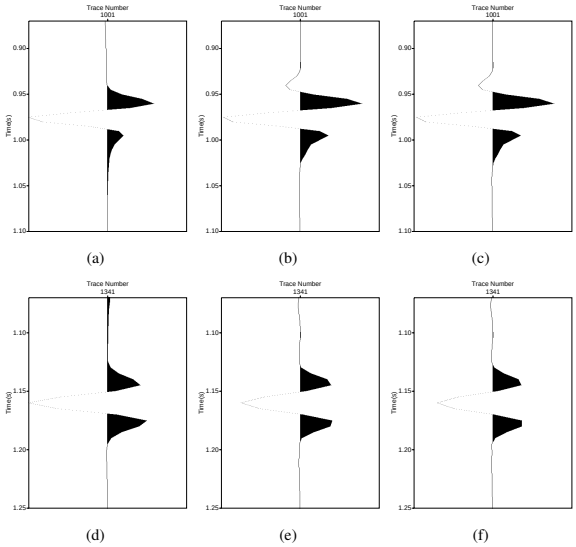

(a) (b) (c)

(d) (e) (f)

Figure 6: (a), (b), (c) The middle traces, and (d), (e), (f) the far traces, picked from the input data and the internal multiples predicted by the ISS IMA algorithm with and without incorporating the source wavelet and radiation pattern.

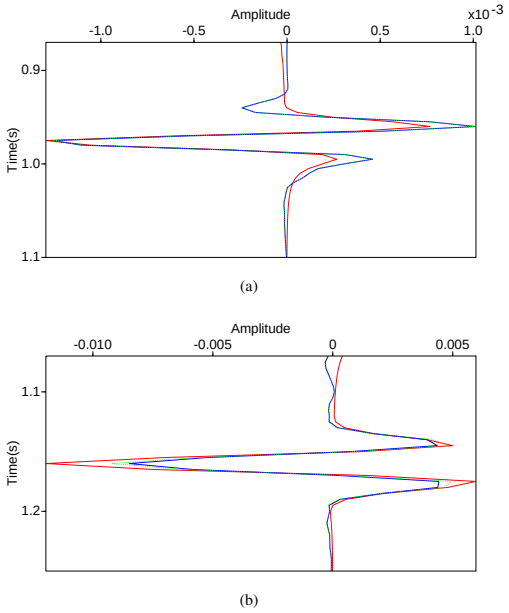

(a)

(b)

Figure 7: The comparison between the true internal multiple (red) in the input data and the internal multiple predicted by the ISS IMA algorithm with (green dash) and without (blue) incorporating the source wavelet and radiation pattern at (a) zero offset and at (b) far offset ($1700m$).

ACKNOWLEDGMENTS

We are grateful to all M-OSRP sponsors for their encouragement and support of this research.

REFERENCES

Araújo, F. V., 1994, Linear and non-linear methods derived from scattering theory: backscattered tomography and internal multiple attenuation: PhD thesis, Universidade Federal da Bahia.

Araújo, F. V., A. B. Weglein, P. M. Carvalho, and R. H. Stolt, 1994, Inverse scattering series for multiple attenuation: An example with surface and internal multiples: 64th Annual International Meeting, SEG, Expanded Abstracts, 1039–1042.

Carvalho, P. M., 1992, Free-surface multiple reflection elimination method based on nonlinear inversion of seismic data: PhD thesis, Universidade Federal da Bahia.

Herrera, W., and A. B. Weglein, 2013, Eliminating first-order internal multiples with downward reflection at the shallowest interface: Theory and initial examples: 83rd International Annual Meeting, SEG, Expanded Abstracts, 4131–4135.

Liang, H., C. Ma, and A. B. Weglein, 2013, General theory for accommodating primaries and multiples in internal multiple algorithm: Analysis and numerical tests: 83rd International Annual Meeting, SEG, Expanded Abstracts, 4178–4183.

Loveridge, M. M., G. E. Parkes, L. Hatton, and M. H. Worthington, 1984, Effects of marine source array directivity on seismic data and source signature deconvolution: First Break, **2**, 16–22.

Matson, K. H., D. C. Corrigan, A. B. Weglein, C. Y. Young, and P. M. Carvalho, 1999, Inverse scattering internal multiple attenuation: results from complex synthetic and field data examples: 69th Annual International Meeting, SEG, Expanded Abstracts, 1060–1063.

Mayhan, J. D., A. B. Weglein, and P. Terenghi, 2012, First application of Green's theorem derived source and receiver deghosting on deep water Gulf of Mexico synthetic (SEAM) and field data: 82nd Annual International Meeting, SEG, Expanded Abstracts, 1–5.

Ramírez, A. C., and A. Weglein, 2005, An inverse scattering internal multiple elimination method: Beyond attenuation, a new algorithm and initial tests: 75th International Annual Meeting, SEG, Expanded Abstracts, 2115–2118.

Tang, L., J. D. Mayhan, J. Yang, and A. B. Weglein, 2013, Using green's theorem to satisfy data requirements of inverse scattering series multiple removal methods: 83rd International Annual Meeting, SEG, Expanded Abstracts, 4392–4396.

Weglein, A. B., F. V. Araújo, P. M. Carvalho, R. H. Stolt, K. H. Matson, R. T. Coates, D. Corrigan, D. J. Foster, S. A. Shaw, and H. Zhang, 2003, Inverse scattering series and seismic exploration: Inverse Problems, R27–R83.

Weglein, A. B., F. A. Gasparotto, P. M. Carvalho, and R. H. Stolt, 1997, An inverse-scattering series method for attenuating multiples in seismic reflection data: Geophysics, **62**, 1975–1989.

Weglein, A. B., and B. G. Secrest, 1990, Wavelet estimation for a multidimensional acoustic earth model: Geophysics, **55**, 902–913.

Yang, J., J. D. Mayhan, L. Tang, and A. B. Weglein, 2013, Accommodating the source (and receiver) array in free-surface multiple elimination algorithm: impact on interfering or proximal primaries and multiples: 83rd International Annual Meeting, SEG, Expanded Abstracts, 4184–4189.

Yang, J., and A. B. Weglein, 2013, Incorporating the source array in the free-surface multiple elimination algorithm: impact on removing a multiple that interferes with a primary and first test of the source deconvolution on the internal multiple attenuation algorithm: M-OSRP Annual Report.

Zhang, J., and A. B. Weglein, 2005, Extinction theorem deghosting method using towed streamer pressure data: Analysis of the receiver array effect on deghosting and subsequent free surface multiple removal: 2095–2100.

Zou, Y., and A. B. Weglein, 2013, A new method to eliminate first order internal multiples for a normal incidence plane wave on a 1d earth: 83rd International Annual Meeting, SEG, Expanded Abstracts, 4136–4140.